Pressure Swing Adsorption Cycles for Improved Solvent Vapor Enrichment

Yujun Liu and James A. Ritter
Dept. of Chemical Engineering, Swearingen Engineering Center, University of South Carolina, Columbia, SC 29208

Bal K. Kaul
Exxon Research and Engineering Company, Florham Park, NJ 07932

A pressure swing adsorption (PSA)–solvent vapor recovery (SVR) process simulator was used to investigate new PSA cycle configurations designed for higher solvent vapor enrichment. These cycles were modifications of the four-step Skarstrom cycle used commercially for PSA-SVR and include the addition of a cocurrent blowdown step, and combinations of cocurrent blowdown and continuous/batch reflux steps. The recovery of gasoline vapor from tank filling operations was simulated with n-butane, n-heptane, and nitrogen as representatives of the light and heavy components in gasoline vapor, and carrier gas, respectively. Adding a cocurrent blowdown step increased the solvent vapor enrichment, depending mainly on the step ending pressure, not the step time. Both the continuous and batch reflux steps also increased the solvent vapor enrichment, but at the expense of an increased bed capacity factor. For similar increases in the solvent vapor enrichment, batch reflux led to significantly smaller bed capacity factors compared to continuous reflux and was thus superior for PSA-SVR. Overall PSA-SVR process performance improved markedly by adding cocurrent blowdown and batch reflux steps compared to the conventional four-step cycle.

Introduction

PSA has established itself as a competitive technology in the important area of SVR. Existing and potential commercial applications include the recovery of many different solvent vapors (Holman and Hill, 1992; Hall and Larrinage, 1993) and hydrocarbon gasoline vapors (Pezolt et al., 1997), with more than 100 gasoline vapor recovery units already operating worldwide. Related theoretical and experimental studies from academia have paralleled this rapidly growing interest in PSA for SVR (Suh and Wankat, 1989a; Ritter and Yang, 1991a,b; LeVan, 1995; Liu and Ritter, 1996; 1998 Pigorini and LeVan, 1997; Liu and Ritter, 1997a,b; Subramanian and Ritter, 1997; Ritter and Liu, 1998; Ritter et al., 1998; Subramanian and Ritter, 1998; Liu et al., 1998a,b; Subramanian et al., 1999; Liu et al., 1999a,b, 2000).

PSA for SVR is different from conventional PSA processes in that the desirable product is a heavy component (or components); however, the purity of the light component (usually air in SVR processes) also has imposed constraints that must be met due to environmental regulations. So the process performance is judged not only by the purity, recovery, and productivity of the light component (like in conventional PSA processes), but also by the enrichment and recovery of the heavy component(s) (Liu and Ritter, 1996). Moreover, almost all of the PSA-SVR processes commercialized so far have utilized the simple, twin-bed, Skarstrom-type cycle (Holman and Hill, 1992; Hall and Larrinage, 1993; Pezolt et al., 1997). While this cycle easily handles feed mixtures to meet the strictest known emission regulations, the enrichment of the heavy component(s) is usually far below the thermodynamic limitation, which is governed by the pressure ratio (Subramanian and Ritter, 1997). Low enrichments necessarily increase the cost of downstream processes designed for reclaiming the heavy components.

Very little effort has been put forth in the development of new PSA cycles that focus on increasing the heavy component enrichment. A few exceptions include the works by Suh

Correspondence concerning this article should be addressed to J. A. Ritter.

and Wankat (1989a,b), Ruthven and Farooq (1994), Ruthven et al. (1994), Diagne et al. (1994, 1995), Betlem et al. (1998), Yoshida et al. (1998), and Dong et al. (1999). Using a local equilibrium model, Suh and Wankat (1989a) showed that if the heavy component mole fraction in the feed is not too high and the relative affinity of the components is not too low, addition of a cocurrent blowdown step has a favorable effect of the light component recovery and heavy component enrichment. Ruthven et al. (1994) also briefly discussed the effect of cocurrent blowdown on the recovery and enrichment of strongly adsorbed species in equilibrium-controlled PSA separation processes. Suh and Wankat (1989b) proposed a new PSA process that employs an inert column between two adsorbent columns for compression and recycling of the strongly adsorbed component streams using the weakly adsorbed component stream. Their equilibrium theory analysis showed that a much higher enrichment of the heavy component can be achieved, depending on the ratio of the volumes of the inert and adsorption columns, the pressure ratio, and the so-called low-pressure cut. Diagne et al. (1994, 1995) developed a PSA process with an intermediate feed inlet that operated with dual refluxes for recovery and enrichment of CO_2 from air. Using experiments, Yoshida et al. (1998) and using simulations, Dong et al. (1999) explored similar PSA processes, respectively, for trace component enrichment and multicomponent separation. The dual reflux steps included a stripping reflux step, which was equivalent to a light product purge, and an enriching reflux step, which involved recycling the effluent during the desorption step. In all cases, these reflux steps allowed for a much higher enrichment of the heavy component(s) compared to conventional PSA processes. Reflux cycles in a three-step, rapid PSA process were also employed by Betlem et al. (1998) for a hypothetical binary mixture.

Clearly, the studies on enhancing the enrichment in PSA-SVR processes are far from sufficient; most of the studies mentioned above involved only oversimplified modeling or hypothetical non-SVR PSA systems. The objective of this research is, therefore, to investigate several PSA cycle configurations, using a rigorous mathematical model and a full-scale, commercially relevant PSA-SVR system. These new, modified Skarstrom-type cycles for SVR include the addition of a cocurrent blowdown step, and combinations of cocurrent blowdown and continuous/batch reflux steps. The PSA-SVR process under investigation simulates the recovery of gasoline vapor from tank filling operations with n-butane, n-heptane, and nitrogen as representatives of the light and heavy vapor components in gasoline vapor and carrier gas, respectively. Both the process performance and process dynamics are used to gain a better understanding of these cycles, and to identify the best configuration for PSA-SVR.

New Cycle Configurations

Most of the commercial PSA-SVR systems have utilized a twin-column, four-step, Skarstrom-type cycle, with the four steps as high-pressure (P_H) (kPa) feed (typically around atmospheric pressure), countercurrent blowdown (evacuation) from P_H to a low vacuum pressure (P_L), countercurrent purge at P_L, and repressurization from P_L to P_H. In essence, PSA-SVR processes are vacuum swing processes due to the strong affinity between the solvent vapor and the adsorbent, which requires very low pressures for desorption and, thus, adsorbent regeneration, and due to the feed in most cases being available at pressures just slightly greater than atmospheric pressure. The three different PSA-SVR cycles investigated here are similar to this vacuum swing Skarstrom-type cycle, but with additional cycle steps for improving heavy component enrichment. The first new PSA-SVR cycle involves the addition of a cocurrent blowdown step between the feed and countercurrent blowdown steps, as shown in Figure 1a. After the high-pressure feed step, the column is depressurized cocurrently for a specified time t_{ce}, to an intermediate pressure (P_{ce}), which falls in-between the values of P_H and P_L. The second new PSA-SVR cycle combines the five-step cocurrent blowdown cycle with continuous reflux of some of the heavy component effluent. This cycle configuration is illustrated in Figure 1b. In this cycle, a certain portion of the effluents from the countercurrent blowdown and purge steps of one column are recycled and mixed continuously with the fresh feed during the high-pressure feed step of the other column. The amount of the effluent taken as reflux is determined by the reflux ratio (R_c), which is defined as the ratio of the reflux flow rate to the effluent flow rate. In principle, there is no limitation on the step times; however, to avoid discontinuities in the flow rates and in the composition of the mixture entering the column during the feed step, this cycle is synchronized to let the feed step time equal the total time of the countercurrent blowdown and purge steps. The third new PSA-SVR cycle is a five-step cycle with the cocurrent blowdown step combined with a batch reflux, as shown in Figure 1c. In this cycle configuration, the effluent from part of the countercurrent blowdown step starting from the beginning of the step ($t = 0$) to an intermediate time $t_{b,i}$, and the effluent from part of the purge step starting from an intermediate time $t_{pu,i}$ to the end of this step ($t = t_{pu}$), are recycled and mixed in a storage tank. This mixture is then continuously added to the fresh feed during the entire feed step of the other column in the next cycle. This idea of using a batch reflux step came from the concentration histories of the effluents during the countercurrent blowdown and purge steps from a typical four-step Skarstrom-type cycle (Liu et al., 1998b). The solvent vapor concentrations always increase with time during the countercurrent blowdown step and decrease with time during the purge step, and the maximum concentrations occur at the end of blowdown and beginning of the purge steps. So, in this new batch reflux cycle, the effluents in the initial stages of the countercurrent blowdown step and final stages of the purge step are recycled, and only the effluents in the final stages of the countercurrent blowdown and initial stages of the purge steps are taken as product. Because of the batch nature of this cycle, there is no limitation on the cycle step times. However, for comparison purposes, the cycle step times are the same as those used in the continuous reflux cycle; also, the fractions of the times of the countercurrent blowdown and purge steps are the same and are denoted by R_b.

Mathematical Model

The PSA process simulator used in this study is similar to the one developed previously by the authors (Liu and Ritter,

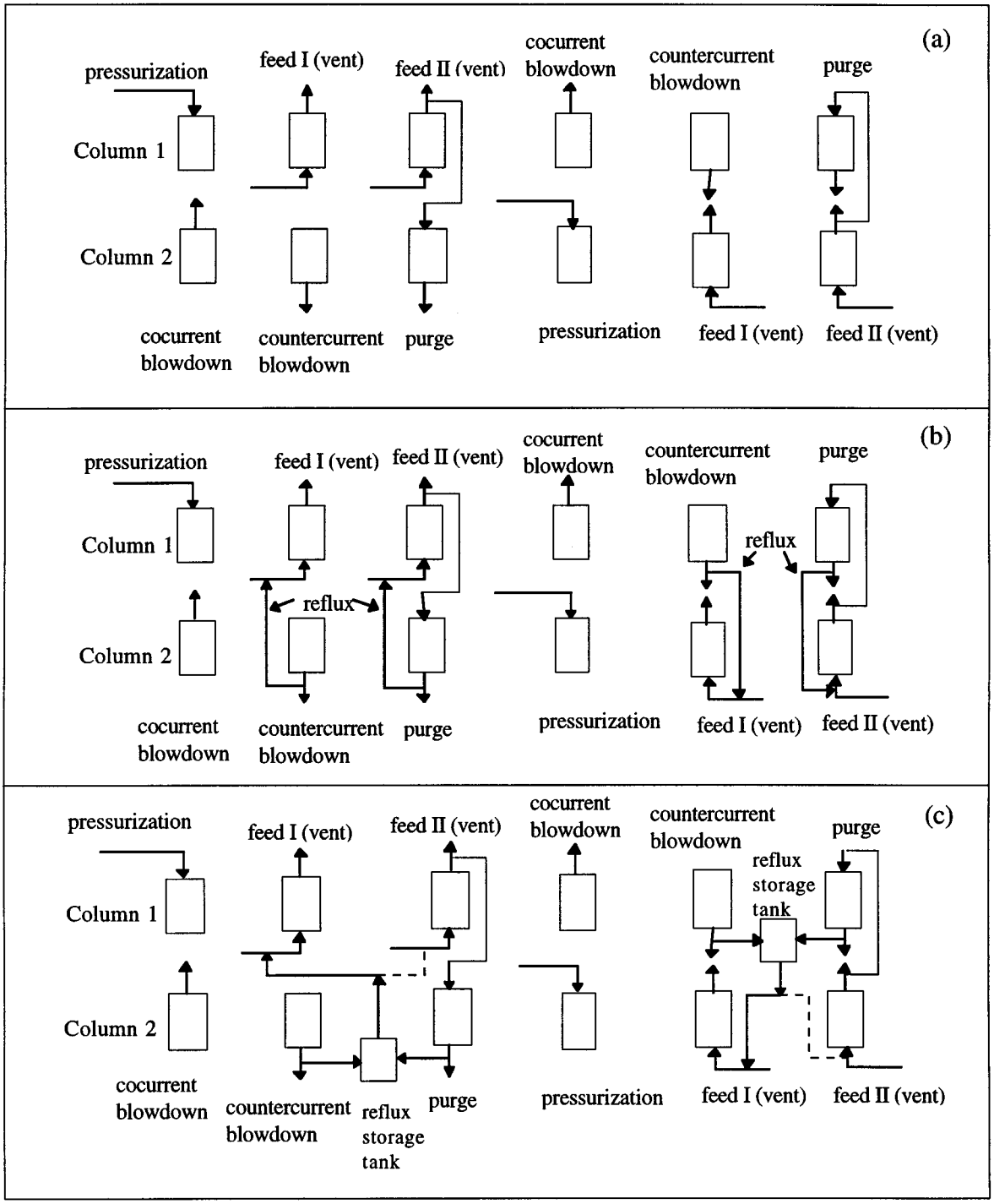

Figure 1. Three different modifications to the four-step, Skarstrom-type cycle for PSA-SVR.

(a) Addition of a cocurrent blowdown step; (b) addition of a cocurrent blowdown step and continuous reflux; (c) addition of a cocurrent blowdown step and batch reflux.

1998; Liu et al., 1999b), except that the present model takes into account the gas-phase capacitance (mass and energy) inside the pores of the adsorbent particles. Although including the gas-phase capacitance inside the pores of the particles has only a minor effect on the dependent variable profiles, it certainly makes the simulator more realistic compared to the previous model. The model also accounts for the temperature-dependence of the gas-phase physical properties, heat capacity of the adsorbed phase, and loading dependence of the heat of adsorption, and assumes some common assumptions that are generally utilized in PSA simulations. These include: ideal gas law, negligible column pressure drop, thermal equilibrium between gas and solid phases, plug flow, negligible axial and radial dispersions, negligible axial heat con-

duction, and temperature-independent adsorbent properties (Yang, 1987; Ruthven et al., 1994; Liu et al., 1999b). Consideration of the gas-phase capacitance inside the pores leads to a few changes in the model equations.

For an N-component PSA-SVR process, the total mass balance is given by

$$\frac{\partial u}{\partial z} - \frac{u}{T}\frac{\partial T}{\partial z} + \frac{\epsilon + (1-\epsilon)(\chi - \varphi)}{\epsilon}\left(\frac{1}{P}\frac{\partial P}{\partial t} - \frac{1}{T}\frac{\partial T}{\partial t}\right) - \frac{1-\epsilon}{\epsilon}\frac{\partial \varphi}{\partial t} + \sum_{i=1}^{N} S_i = 0 \quad (1)$$

where χ is the porosity of the adsorbent particle and φ is the pore volume occupied by the adsorbed phase per particle volume and is calculated from

$$\varphi = \sum_{i=1}^{N} \frac{q_i \rho_p M_i}{\rho_{ai}} \quad (2)$$

ρ_{ai} is the density (kg/m^3) of the ith adsorbed phase and approximated from the corresponding density of the saturated liquid. S_i in Eq. 1 is expressed as

$$S_i = \frac{1-\epsilon}{\epsilon}\frac{RT\rho_p}{P}\frac{\partial q_i}{\partial t} \qquad i = 1, 2, \ldots, N \quad (3)$$

and $\partial q_i/\partial t$ is based on the LDF approximation as

$$\frac{\partial q_i}{\partial t} = k_i(q_i^* - q_i) \qquad i = 1, 2, \ldots, N \quad (4)$$

The component mass balances are given by

$$\frac{\epsilon + (1-\epsilon)(\chi - \varphi)}{\epsilon}\frac{\partial y_i}{\partial t} + u\frac{\partial y_i}{\partial z} - y_i\sum_{j=1}^{N} S_j + S_i = 0 \qquad i = 1, 2, \ldots, N-1 \quad (5)$$

and the energy balance is expressed as

$$Cp_g\frac{\partial T}{\partial t} + uCp_g\frac{\partial T}{\partial z} + \rho_p Cp_p\frac{1-\epsilon}{\epsilon}\frac{RT}{P}\frac{\partial T}{\partial t} + \frac{1-\epsilon}{\epsilon}\frac{RT}{P}\rho_p\sum_{i=1}^{N}\left(Cp_{ai}q_i\frac{\partial T}{\partial t} + \Delta H_i\frac{\partial q_i}{\partial t}\right) + \frac{2h}{\epsilon r_b}\frac{RT}{P}(T - T_o) = 0 \quad (6)$$

The gas-phase heat capacity is given by

$$Cp_g = \sum_{i=1}^{N} y_i Cp_{gi} \quad (7)$$

where

$$Cp_{gi} = A_i + B_iT + C_iT^2 + D_iT^3 \qquad i = 1, 2, \ldots, N \quad (8)$$

The single component equilibrium amounts adsorbed are represented by the three process Langmuir model (Drago et al., 1996; Liu et al., 1999b, 2000), which is modified for mixtures as

$$q_i^* = \sum_{j=1}^{3}\frac{q_{i,j}^s b_{i,j} P y_i}{1 + \sum_{i=1}^{N} b_{i,j} P y_i} \qquad i = 1, 2, \ldots, N \quad (9)$$

where

$$b_{i,j} = b_{i,j}^o \exp\left(\frac{B_{i,j}}{T}\right) \quad (10)$$

In all cases, the simulations begin with clean beds (beds filled with nitrogen at P_H). The initial conditions of each step in the subsequent cycle steps are those at the end of the previous step. For the four and five step processes not utilizing reflux, the initial and boundary conditions employed are summarized in Table 1. For the feed step of the cycle with continuous reflux, the mixture composition at the column inlet is taken as the volume-averaged mole fractions of the fresh feed and the reflux at time t. The inlet flow rate is the sum of the fresh feed and the reflux at that time. Therefore, the boundary conditions are: $z = 0$ for all $t > 0$

$$y = \frac{y_{f,i}V_f^o + y_{e,i}V_{e,b(\text{or } pu)}^o}{V_f^o + V_{e,b(\text{or } pu)}^o} \quad (11)$$

$$u = \frac{V_f^o + V_{e,b(\text{or } pu)}^o}{A\epsilon} \times \frac{P^oT_f}{P_HT^o} \quad (12)$$

$$T = T_f \quad (13)$$

Table 1. Initial and Boundary Conditions for the Four and Five Step PSA-SVR Processes Not Utilizing Reflux*

Pressurization Step (I)				
at $t = 0$:	$y_i = y_{i,\text{IV}}$,	$T = T_{\text{IV}}$	$q_i = q_{i,\text{IV}}$,	for all z
at $z = 0$:	$u = 0$			for all t
at $z = L$:	$y_i = 0$,	$y_N = 1$,	$T = T_0$, $i = 1 \ldots N-1$	for all t
Feed Step (II)				
at $t = 0$:	$y_i = y_{i,\text{I}}$,	$T = T_1$,	$q_i = q_{i,1}$,	for all z
at $z = 0$:	$y_i = y_{i,f}$,	$T = T_f$,	$u = u_f$	for all t
Cocurrent Blowdown Step (III)				
at $t = 0$:	$y_i = y_{i,\text{II}}$,	$T = T_{\text{H}}$,	$q_i = q_{i,\text{II}}$,	for all z
at $z = 0$:	$u = 0$			for all t
Countercurrent Blowdown Step (IV)				
at $t = 0$:	$y_i = y_{i,\text{III}}$,	$T = T_{\text{III}}$,	$q_i = q_{i,\text{III}}$,	for all z
at $z = L$:	$u = 0$			for all t
Purge Step (V):				
at $t = 0$:	$y_i = y_{i,\text{IV}}$,	$T = T_{\text{IV}}$,	$q_i = q_{i,\text{IV}}$,	for all z
at $z = L$:	$y_i = y_{i,\text{II}}$ (t),	$T = T_{\text{II}}$ (t),	$u = u_{\text{P}}$	for all t

*i varies from 1 to N if not otherwise specified.

Note that the superscript o denotes standard temperature and pressure, and both $y_{e,i}$ and V_e^o are time-dependent. For the feed step of the cycle with batch reflux, it is assumed that the reflux in the storage tank from the previous cycle is uniformly mixed and equally distributed to the column undergoing the high-pressure feed step of the present cycle. The mixture composition at the column inlet is taken as the volume-averaged mole fractions of the fresh feed and reflux in the storage tank using the total volume fed to the column during the entire step and the total volume of the reflux fed to the storage tank in the previous cycle. So, the boundary conditions are: at $z = 0$ for all $t > 0$

$$y = \frac{y_{f,i} V_f^o t_f + \int_0^{t_{b,i}} y_{e,b,i} V^o{}_{e,b}\, dt + \int_{t_{pu,i}}^{t_{pu}} y_{e,pu,i} V^o{}_{e,pu}\, dt}{V_f^o t_f + \int_0^{t_{b,i}} V_{e,b}^o\, dt + \int_{t_{pu,i}}^{t_{pu}} V_{e,pu}^o\, dt} \quad (14)$$

$$u = \frac{V_f^o t_f + \int_0^{t_{b,i}} V^o{}_{e,b}\, dt + \int_{t_{pu,i}}^{t_{pu}} V^o{}_{e,pu}\, dt}{A\epsilon} \times \frac{P^o T_f}{P_H T^o} \quad (15)$$

$$T = T_f \quad (16)$$

Equations 1 to 10, along with the set of initial and boundary conditions, represent the comprehensive mathematical model of a multicomponent PSA-SVR process. This model is solved using a robust PSA process simulator developed by the authors that is based on a finite difference technique coupled with a time-adaptive DAE solver called DASPK (Brown et al., 1994).

The pressure in the pressure-changing steps is taken as a linear function of time, and it is fixed at P_H and P_L during the feed and purge steps, respectively. Because of the large scale of the PSA system, only adiabatic conditions are simulated; therefore, the overall heat-transfer coefficient (h) (kJ/m^2·s·k) is set to zero in all cases. The accuracy of the PSA process simulator has been validated with extensive experimental data obtained from a highly nonisothermal bench-scale PSA-SVR system (Liu et al., 1999b), and, thus, it should be fairly accurate in simulating a large-scale system under the adiabatic condition. The mass-transfer coefficients and the adsorbed phase heat capacities are taken from our previous studies (Liu and Ritter, 1998; Liu et al., 1999b); all of the values are given in Table 2. The coefficients in the gas-phase heat capacity correlation, the adsorption isotherm model, and the correlation for the heat of adsorption are tabulated in Table 3.

Results and Discussion

The specific PSA-SVR system under investigation is a full-scale system, with the column dimensions being typical of a PSA-gasoline vapor recovery process. The column characteristics are given in Table 2. The feed mixture contains 25% *n*-butane, 1% *n*-heptane, and the balance nitrogen; these heavy component compositions are typical of gasoline vapor (Pezolt et al., 1997). In all cases, P_H is 135.3 kPa and P_L is 10 kPa, and the total cycle time is fixed at 30 min, except for the processes used to investigate the effect of the cocurrent blowdown step time. Moreover, to meet the tough environmental regulations on gasoline vapor emissions, the PSA processes investigated have been designed to produce essentially solvent-free light product, that is, no butane and heptane vapors are present in the light product streams of the feed and cocurrent blowdown steps, and the recoveries of these vapors are 100%, unless otherwise noted. Under these circumstances, the process performance is judged solely in terms of the solvent vapor enrichment (E) and the bed capacity factor (BCF) (Liu and Ritter, 1996), which are defined for each component as the average solvent vapor mole fraction in the effluent streams divided by the solvent vapor mole fraction in the feed, and the total amount adsorbed in the column at the end of the feed step divided by the equilibrium amount adsorbed in the entire column at the feed conditions, respectively. The BCF represents the extent to which the adsorbent has been contaminated with solvent vapors; therefore, under

Table 2. Column Characteristics and Base Case Operating Conditions for the PSA-SVR Processes

Column Characteristics		Operating Conditions	
r_b (m)	1.525	$y_{f,\mathrm{bu}}$	0.25
L (m)	3.658	$y_{f,\mathrm{hep}}$	0.01
ρ_p (kg/m^3)	550.0	$y_{f,\mathrm{nit}}$	0.76
ϵ (−−)	0.391	P_H (kPa)	135.8
Cp_p (kJ/kg·K)	1.046	P_L (kPa)	10.0
Cp_a (C_4H_{10}) (kJ/mol·K)	9.86×10^{-2}	γ	1.35
		t_c (min)	30.0
Cp_a (C_7H_{16}) (kJ/mol·K)	9.22×10^{-2}	t_{pres} (min)	3.0
Cp_a (N_2) (kJ/mol·K)	2.84×10^{-2}	t_f (min) (II, III)	12.0
k_i (s^{-1})	0.02699	T_f (K)	302.6
h (kJ/m^2·s·K)	0.0	T_o (K)	298.0

Table 3. Values of the Parameters used in the PSA-SVR Process Simulator

	Parameters for the Gas-Phase Heat Capacity, Cp_g (kJ/(mol·K))			
	A$\times10^2$	B$\times10^4$	C$\times10^7$	D$\times10^{11}$
n-Butane	0.948	3.310	−1.107	−0.282
n-Heptane	2.348	1.723	3.144	−39.84
Nitrogen	3.112	−0.136	0.268	1.167

	Parameters for the Three Process Langmuir Model*			
		q_m	b_0	B
n-Butane-BAX	Process 1	6.4627	1.5091×10^{-8}	3968.5822
	Process 2	2.6820	7.2187×10^{-8}	4653.4317
	Process 3	0.7305	5.3529×10^{-8}	6009.3764
n-Heptane-BAX	Process 1	7.3252	6.4110×10^{-7}	3587.2287
	Process 2	2.5847	8.9100×10^{-6}	4349.8245
	Process 3	0.5412	3.8800×10^{-5}	5153.0067
Nitrogen-BAX	Process 1	1.2163	6.8751×10^{-5}	720.8872
	Process 2	2.1379	4.2256×10^{-8}	2552.3570
	Process 3	0.0189	2.0223×10^{-33}	21347.0611

	Coefficients for the Isosteric Heat of Adsorption, ΔH (kJ/mol)				
	c_0	c_1	c_2	c_3	c_4
n-Butane	−53.879	14.446	−4.753	0.744	−0.041
n-Heptane	−62.76	0.0	0.0	0.0	0.0
Nitrogen	−44.105	55.222	366.376	−1706.729	1831.5

*Liu et al. (2000).

the same process conditions and performance, a smaller BCF is desirable. A PSA-SVR process utilizing the four-step, Skarstrom-type cycle is used as a basis for evaluating the performances of the PSA-SVR processes utilizing the new cycles.

Effect of cocurrent blowdown

Five runs were used to investigate the effect of the cocurrent blowdown step time (t_{ce}) at a fixed blowdown end pressure of 62.92 kPa. To ensure that the effect obtained was solely that of the cocurrent blowdown step, the time of this step was added to the cycle time of the four-step, Skarstrom-type cycle, which had a total cycle time of 30 min with 12, 9, 6, and 3 min for the feed, countercurrent blowdown, purge and pressurization steps, respectively. The t_{ce} was added to the 30 min and varied from zero to four min in one min increments. The other process conditions were the same as those of the base case given in Table 2. In all of these runs, no solvent vapor breakthrough occurred during the feed and cocurrent blowdown steps.

Figure 2 shows the percentage increases of the solvent vapor enrichment and bed capacity factor for the processes utilizing a cocurrent blowdown step compared to those of the four-step process. Adding a cocurrent blowdown step increased both the butane and heptane vapor enrichments by about 25%, which was a favorable effect; however, it also increased the bed capacity factors of both butane and heptane by about 25% and 10%, respectively, which was an unfavorable effect. Moreover, increasing t_{ce} beyond about 1 min had little effect on further improving the process performance in terms of the enrichments; in contrast, the BCF of both components continued to increase rather markedly with an increase in t_{ce}.

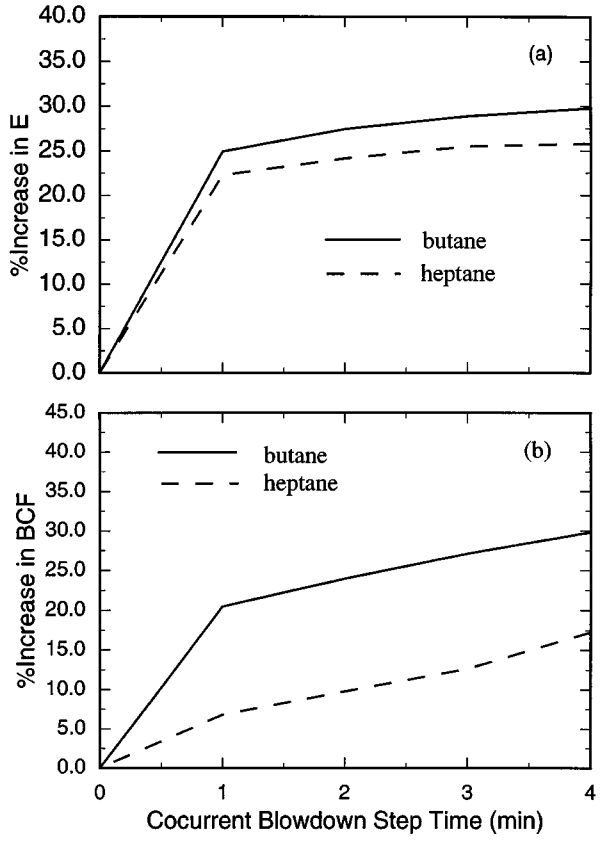

Figure 2. Effect of the cocurrent blowdown step time (t_{ce}) on the (a) solvent vapor enrichment and (b) bed capacity factor relative to the four-step cycle with $t_{ce} = 0$ min $P_{ce} = 62.92$ kPa in the five-step cycles.

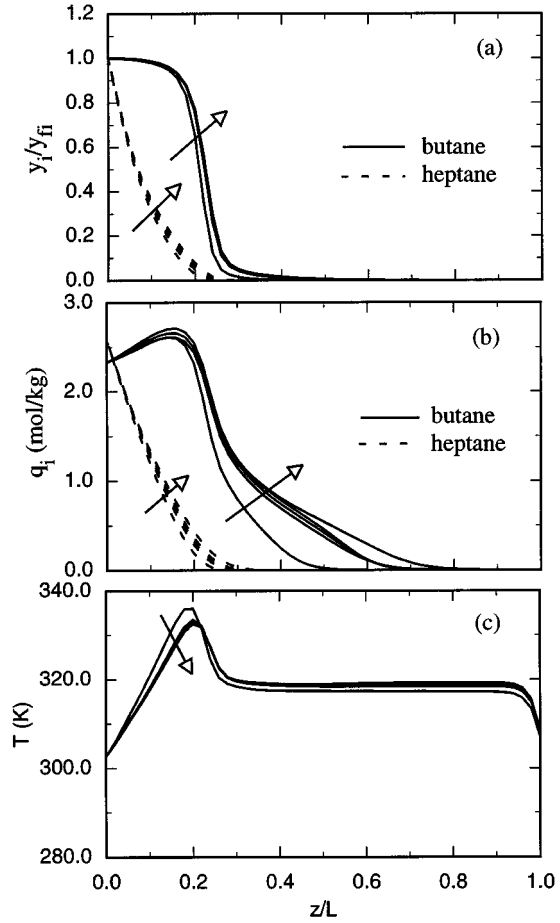

Figure 3. Effect of the cocurrent blowdown step time (t_{ce}) on the (a) gas-phase concentration, (b) adsorbed phase concentration, and (c) temperature profiles.

Arrows indicate direction of t_{ce} increasing with t_{ce} equal to 0, 1, 2, 3, 4 min.

Figure 3 displays the gas-and solid-phase concentration and temperature profiles at the end of the adsorption step for all five runs. There was hardly any difference in the gas-phase concentration profiles for these processes, especially for the runs utilizing a cocurrent blowdown step. The adsorbed-phase concentration profiles for heptane also did not change much, which was consistent with the marginal increase in the BCF for heptane. However, the adsorbed-phase concentration profiles for butane in the five-step cycle exhibited marked changes relative to that of the four-step cycle; this corresponded to the rather significant increases in the BCFs for butane up to about 30%. Nevertheless, adding a cocurrent

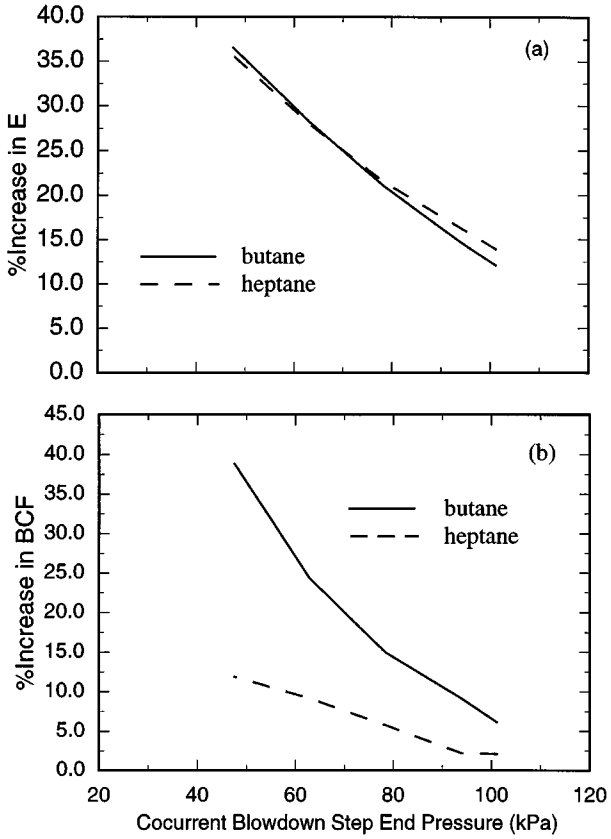

Figure 4. Effect of the cocurrent blowdown step end pressure (P_{ce}) on the (a) solvent vapor enrichment and (b) bed capacity factor relative to the four-step cycle with t_{ce} = 0 min and E_{bu} = 1.778, E_{hep} = 2.249, BCF_{bu} = 0.301 and BCF_{hep} = 0.098. t_{ce} = 3 min in the five-step cycle.

blowdown step to the four-step cycle had only a minimal impact on the heat effects in the column, as shown by the temperature profiles; this was a favorable effect and is discussed in more detail below (Liu and Ritter, 1998).

Five runs were also carried out to investigate the effect of the cocurrent blowdown step end pressure (P_{ce}) with the cycle time fixed at 30 min, that is, at the base case, four-step cycle time. However, the countercurrent blowdown step was split into cocurrent and countercurrent blowdown steps, with the duration of the cocurrent blowdown step fixed at 3 min. Thus, the countercurrent blowdown step was fixed at 6 min. All of the other process conditions were the same as the based conditions given in Table 2. Note that no solvent vapor breakthrough occurred in any of these runs.

Figure 4 shows the percentage increases of the solvent vapor enrichment and bed capacity factor for the processes utilizing different cocurrent blowdown end pressures (P_{ec}) compared to those of the four-step process. Decreasing the cocurrent blowdown end pressure caused significant and similar increases in the butane and heptane vapor enrichments, with percentage increases ranging from 15 to 35%. These were quite favorable effects. However, the bed capacity factors also increased when decreasing the cocurrent blowdown end pressure, especially for butane, which ranged from 10 to 40%. In contrast, the effect was much less on the bed capacity factor for heptane and ranged from only 2 to 12%. Nevertheless, these increases in the BCFs were both unfavorable effects. It was interesting that when P_{ce} was set to atomspheric pressure, the enrichments for both the butane and heptane vapors still increased by about 13%, with only minor increases in the bed capacity factors of both components. This was a very favorable result since no extra energy would be needed to implement such a cocurrent blowdown step in a PSA-SVR process.

Decreasing P_{ce} had little effect on the gas-phase concentration and temperature profiles, similar to the effect of the cocurrent blowdown step time shown in Figure 3. However, the adsorbed-phase concentration profiles show a much more pronounced effect for butane, which was consistent with the marked increases in bed capacity factor shown in Figure 4. These effects were again similar to that shown in Figure 3 for the effect of the cocurrent blowdown step time.

It was interesting that the effects of changing both the cocurrent blowdown step time and end pressure had minimal effects of the temperature profiles. Based on the work by Liu and Ritter (1998), which showed that higher column temperatures in the PSA-SVR give rise to marked increases in the bed capacity factor, suggested that the increases in the bed capacity factor observed in this work were caused solely by desorption coupled with convection. Increasing t_{ce} at a fixed P_{ce} allowed more time for the solvent vapors to desorb; similarly; decreasing P_{ce} at a fixed t_{ce} allowed more desorption to occur based on the corresponding decrease in the capacity of the absorbent. In both cases, the desorbed vapors filled the void space in the column and were subsequently convected toward the light product end of the column. This desorption and convection of the solvent vapors in the cocurrent direction also swept more carrier gas out of the column, which in turn increased the concentration of the solvent vapors that were recovered during the subsequent countercurrent blowdown and purge steps.

Effect of continuous reflux

The only new operating parameter in the continuous reflux cycle was the reflux ratio (R_c); therefore, the same five-step cycle and cycle step times were used as in the P_{ce} investigation. Other process conditions were the same as those of the base case (Table 2). Two sets of simulations were carried out under two different P_{ce}'s (101.3 and 62.92 kPa); each set had six runs and the first run in each set did not use reflux (R_c = 0.0). Note that trace butane vapor breakthrough occurred in three of the twelve runs. In the process with $R_c = 0.5$ and $P_{ce} = 62.92$ kPa, the average butane vapor mole fraction in the light product ($y_{p,\,bu}$) was 20 ppm, which reduced the butane vapor recovery (R_{bu}) to 99.992%. Also, with $R_c = 0.6$ and $P_{ce} = 101.3$ kPa, $y_{p,\,bu} = 10$ ppm and $R_{bu} = 99.995\%$; and with $R_c = 0.6$ and $P_{ce} = 62.92$ kPa, $y_{p,\,bu} = 50$ ppm and $R_{bu} = 99.983\%$.

Figure 5 shows the percentage increases in the solvent vapor enrichment and bed capacity factor of these processes compared with the process without reflux (with $R_c = 0.0$). Increasing the continuous reflux ratio caused the enrichments and the bed capacity factors of both components to increase

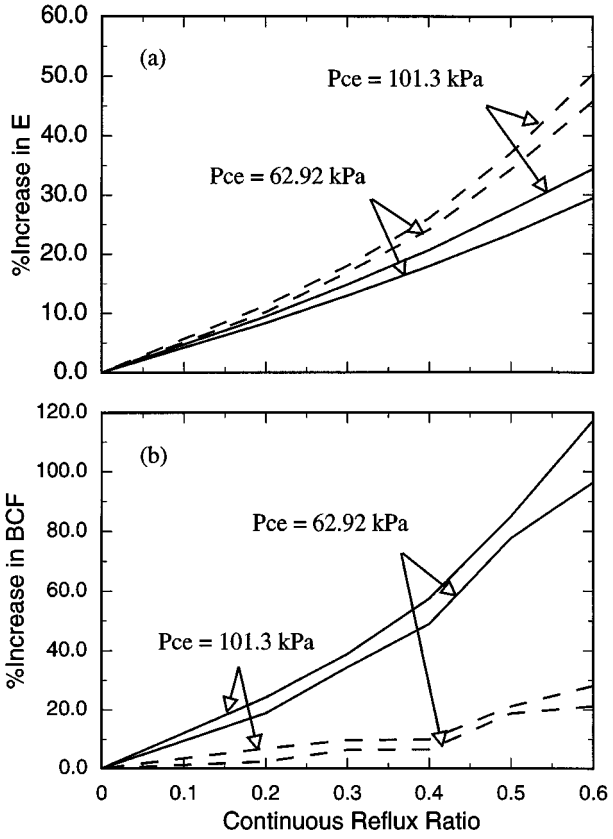

Figure 5. Effect of the continuous reflux ratio (R_c) on the (a) solvent vapor enrichment and (b) bed capacity factor relative to the five-step cycle without reflux.

With $R_c = 0.0$ and $P_{ce} = 101.3$ kPa: $E_{bu} = 1.992$, $E_{hep} = 2.562$, $BCF_{bu} = 0.319$ and $BCF_{hep} = 0.102$. With $R_c = 0.0$ and $P_{ce} = 62.92$ kPa, $E_{bu} = 2.281$, $E_{hep} = 2.880$, $BCF_{bu} = 0.374$ and $BCF_{hep} = 0.105$. Solid lines: butane; dash lines: heptane.

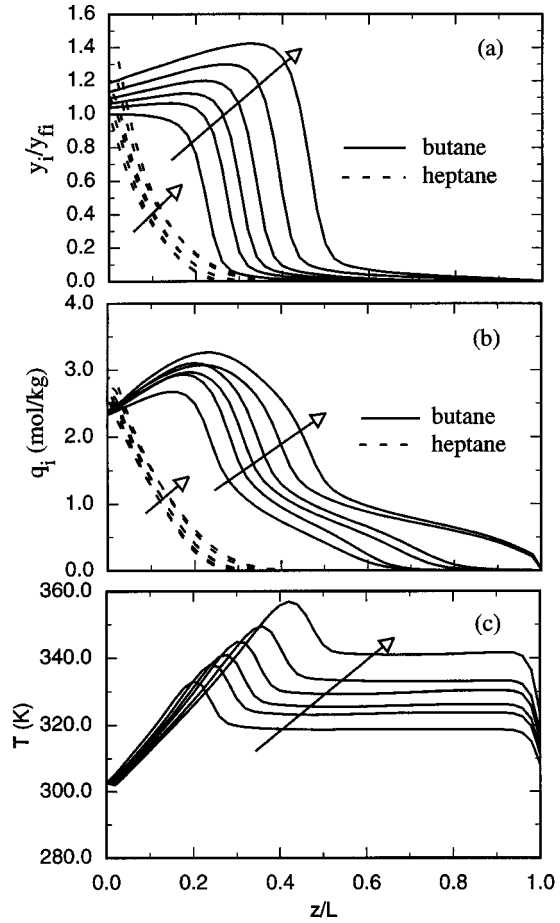

Figure 6. Effect of the continuous reflux ratio (R_c) on the (a) gas-phase concentration, (b) adsorbed-phase concentration and (c) temperature profiles with $P_{ce} = 62.92$ kPa.

Arrows indicate direction of R_c increasing with R_c equal to 0, 0.2, 0.3, 0.4, 0.5 and 0.6.

significantly. The effects were also slightly more pronounced at the higher P_{ce}, as expected based on the trends that were reported in the preceding section. The percentage increases in the enrichment were also consistently larger for heptane than butane, exceeding 50% for the former and only reaching about 35% for the later at the higher P_{ce}. However, the percentage increases in the bed capacity factor for butane were far greater than that for heptane and more than double that obtained with $R_c = 0.0$; in contrast, heptane exhibited only moderate increases in the bed capacity factor of around 25%.

Figure 6 displays the bed profiles for R_c varying from 0.0 to 0.6 and with $P_{ce} = 62.92$ kPa. The gas-phase concentration, adsorbed-phase concentration, and temperature profiles were all dramatically affected by the continuous reflux ratio, except for the heptane profiles. The high capacity of the BAX carbon for heptane vapor prevented the spread of the heptane profiles; it also allowed for minimal breakthrough of butane in the light product stream. This effect is observed most readily from the gas-phase concentration profiles for butane. In the worst case, the leading edge of the knee of the profile only penetrated about half-way through the bed at the end of the feed step, and, thus, even in this worst case, less than 50 ppm of butane was present in the light product effluent. Furthermore, only three of the twelve simulations resulted in any butane breakthrough at all, even though there were marked temperature increases with increasing R_c that definitely contributed to the movement of the butane wavefronts down the column (Liu and Ritter, 1998). These results suggest that continuous reflux could be used to markedly improve the enrichment of the solvent vapors, while still producing a very high-purity light product stream.

Figure 7 shows the percentage increases in the solvent vapor enrichment and bed capacity factor of the continuous reflux PSA processes relative to the basic four-step Skarstrom-type cycle without reflux. Clearly, the use of a cocurrent blowdown step coupled with continuous reflux greatly improved the performance of this PSA-SVR process in terms of the solvent vapor enrichment; but, the improvement came at a cost in terms of the increased bed capacity factor. For example, percentage increases in the enrichment, exceeding 60 to 80% for butane and heptane, respectively, were achieved, but at the expense of the percentage increase in the bed capacity factor for butane exceeding 140%. Nevertheless, for

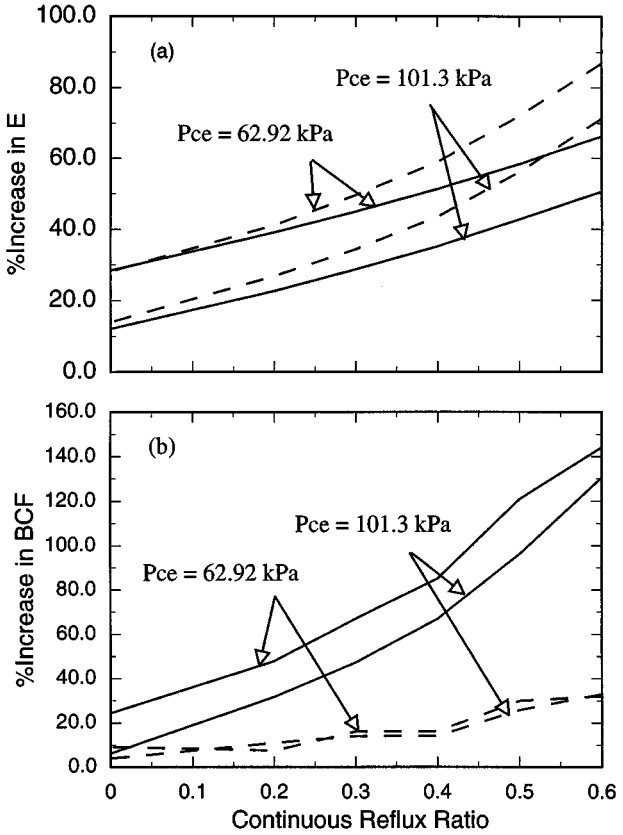

Figure 7. Effect of the continuous reflux ratio (R_c) on the (a) solvent vapor enrichment and (b) bed capacity factor compared with the four-step cycle without reflux and with $E_{bu} = 1.778$, $E_{hep} = 2.249$, $BCF_{bu} = 0.301$ and $BCF_{hep} = 0.098$.

Solid lines: butane; dash lines: heptane.

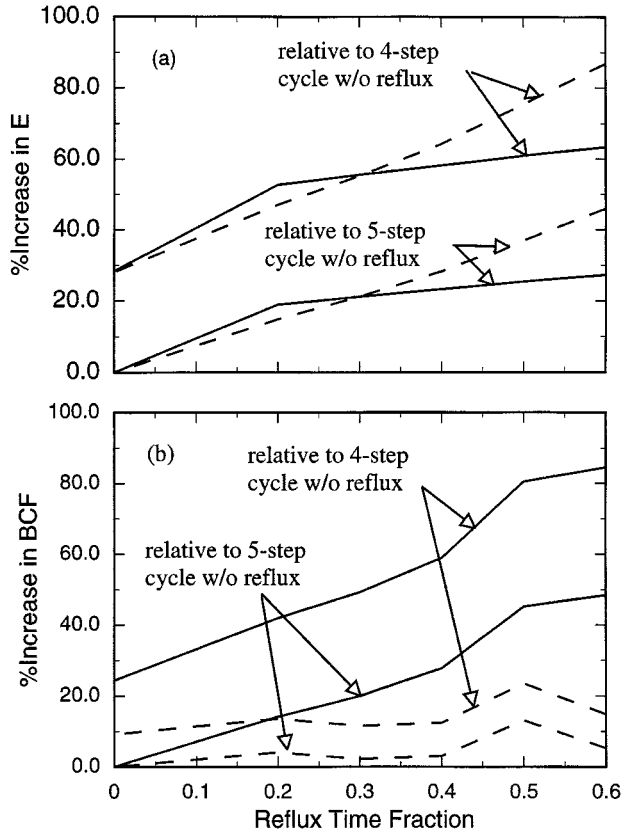

Figure 8. Effect of the batch reflux time fraction (R_b) on the (a) solvent vapor enrichment and (b) bed capacity factor relative to the four and five-step cycles without reflux.

In the four-step cycle without reflux: $E_{bu} = 1.992$, $E_{hep} = 2.562$, $BCF_{bu} = 0.319$ and $BCF_{hep} = 0.102$; in the five-step cycle without reflux: $E_{bu} = 2.281$, $E_{hep} = 2.880$, $BCF_{bu} = 0.374$ and $BCF_{hep} = 0.105$. $P_{ce} = 62.92$ kPa in the five-step cycle.

Solid lines: butane; dash lines: heptane.

properly sized columns, which would necessarily be longer than those required by the four-step cycle, this improved performance could be achieved without sacrificing on the purity of the light product stream.

Effect of batch reflux

The only new operating parameter in the batch reflux cycle is the reflux time fraction (R_b); therefore, six runs were carried out using the same five-step cycle and cycle step times as those used in the continuous reflux investigation. The cocurrent blowdown step ending pressure (P_{ce}) was fixed at 62.92 kPa; all of the other process conditions were the same as those of the base case (Table 2). In all six runs, no butane and heptane vapor breakthrough occurred during the feed or cocurrent blowdown steps.

Figure 8 shows the percentage increases in the solvent vapor enrichment and bed capacity factor relative to that using the same cycle steps without reflux (with $R_b = 0.0$) and relative to that using only four cycle steps without reflux (with $t_{ce} = 0.0$ min and $R_b = 0.0$). Increasing the batch reflux time fraction caused increases in the enrichments of both components, with best case percentage increases of nearly 90% for heptane and over 60% for butane relative to the four-step cycle. The trends were nearly identical relative to the five-step cycle, but with less pronounced results, as expected. This comparison between the four-and five-step cycles also very clearly shows the marked and positive effect of adding a cocurrent blowdown step to a PSA-SVR process. The trends were somewhat different for the bed capacity factor, however. Upon increasing the batch reflux time fraction, the bed capacity factor for butane increased consistently; in contrast, that for heptane was essentially independent of the batch reflux time fraction with the percentage increases hovering around 10% or less relative to the four-step cycle, except at $R_b = 0.5$. These trends were also the same for both the four and five-step cycles, but with less pronounced effects, similarly to the enrichments. In the worst case, the percentage increase in the bed capacity factor for butane, relative to the four-step cycle was around 85%, and around 50% relative to the five-step cycle. What was interesting about these results is that the continuous and batch reflux cycles performed similarly with respect to the enrichments (compare Figures 5a and 7a with Figure 8a), but not with respect to the bed capac-

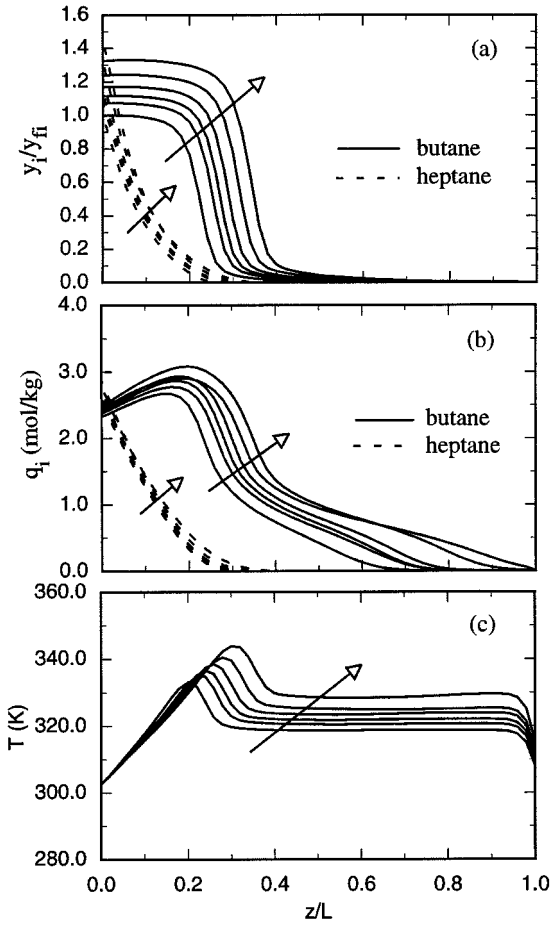

Figure 9. Effect of the batch reflux time fraction (R_b) on the (a) gas-phase concentration, (b) adsorbed-phase concentration and (c) temperature profiles in the processes with a P_{ce} = 62.92 kPa.

Arrows indicate direction of R_b increasing with R_b equal to 0, 0.2, 0.3, 0.4, 0.5 and 0.6.

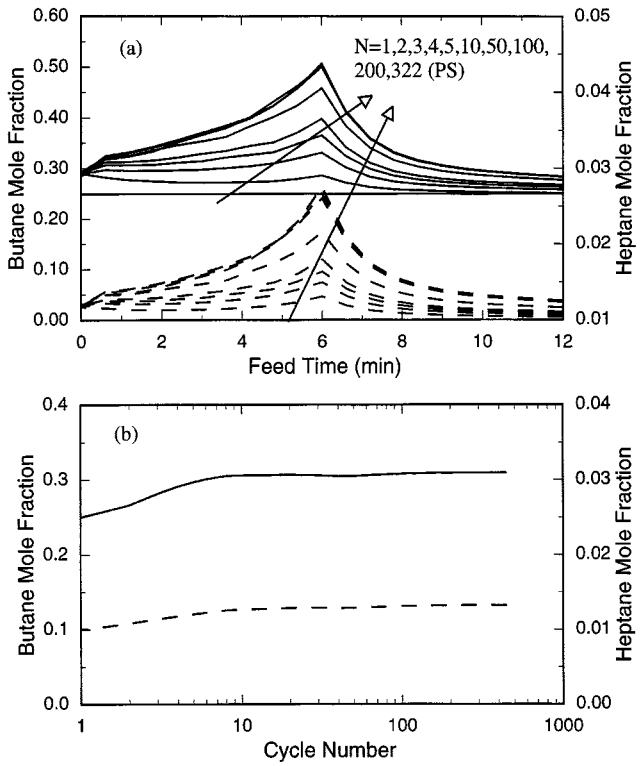

Figure 10. Transient state feed inlet mole fractions of butane and heptane vapors in the five-step PSA cycle with (a) continuous reflux, and R_c = 0.5 and P_{ce} = 62.92 kPa and (b) batch reflux, and R_b = 0.5 and P_{ce} = 62.92 kPa.

Solid lines: butane, dash lines: heptane. N is the cycle number and PS denotes the periodic state.

ity factors. The increases in the bed capacity factor for batch reflux were significantly smaller than those for continuous reflux, especially for butane. For example, at a reflux time fraction of 0.6, the bed capacity factor increased 48.4% for heptane and 84.5% for butane compared to the four-step cycle. In the continuous reflux cycle with $R_c = 0.6$, these increases were 96.3% and 144.1%, respectively. Moreover, while batch reflux produced pure light product during the feed and cocurrent blowdown steps, continuous reflux resulted in butane vapor breaking through the column because of the larger increases in the bed capacity factor of butane.

Figure 9 shows the gas-phase concentration, adsorbed-phase concentration, and temperature profiles at the end of the adsorption step for these batch reflux processes. Increasing R_b pushed the gas-phase concentration, adsorbed-phase concentration, and temperature waves toward the light product end of the column. Moderate temperature increases were also realized with increasing R_b. However, the movements and magnitudes of these waves were not nearly as large as those in the continuous reflux cycles when R_c was increased from 0.0 to 0.6 (compare Figure 9a with 6a, and Figure 9b with 6b). Since both the gas- and adsorbed-phase concentrations in the region close to the light product end of the column (such as $z/L > 0.6$) were considerably lower with batch reflux than with continuous reflux at corresponding values of R_b and R_c, batch reflux resulted in cleaner columns than continuous reflux. These differences in the two kinds of reflux processes were caused by differences in both the inlet feed mole fractions and column throughputs.

Figure 10a shows a very interesting consequence of continuous reflux for the run with $R_c = 0.5$ and $P_{ce} = 62.92$ kPa; the butane and heptane vapor mole fractions at the colum inlet during the feed step not only changed with time during a cycle, but they also increased significantly with the cycle number until the periodic state (PS) was reached. These profiles also peaked at around 6 min into the feed step, and, at the periodic state, the peaks of both components were more than twice those of the fresh feed. In contrast, Figure 10b displays the transient butane and heptane vapor mole fractions at the column inlet during the feed step for the batch reflux process with $R_b = 0.5$. Note that for batch reflux, the mixture composition at the column inlet was constant during the feed step of any cycle. In this case, the butane and heptane mole fractions also increased but only slightly as the periodic state was approached. A comparison between the transient feed concentration histories for the two different reflux

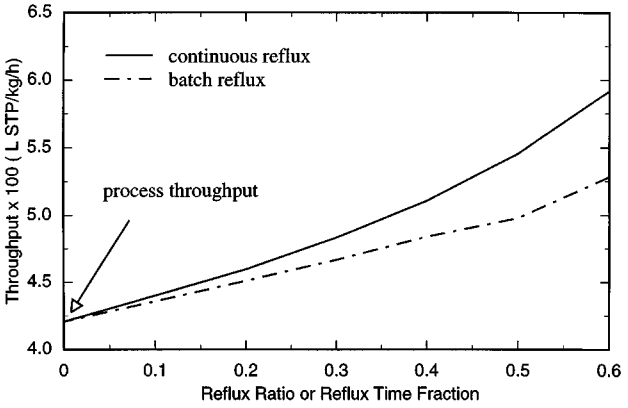

Figure 11. Periodic state column throughputs in the five-step PSA cycle with either continuous or batch reflux, and P_{ce} = 62.92 kPa.

processes shows that the periodic state butane and heptane vapor mole fractions at the feed inlet in the batch reflux process were considerably smaller than those in the continuous reflux process, at least during most of the feed step. Clearly, the higher feed inlet concentrations associated with continuous reflux resulted in larger bed capacity factors and thus contributed to the poorer performance of continuous reflux compared to batch reflux. Moreover, because only the effluents with higher solvent vapor mole fractions were taken as heavy products during the countercurrent blowdown and purge steps in the batch reflux process, the enrichments of the butane and heptane vapors were comparable to the levels obtained with the continuous reflux process. This was a real advantage.

Figure 11 compares the column throughputs from the batch and continuous reflux processes. The column throughput was defined as the combined volume of the fresh feed and the recycled effluent processed per unit adsorbent per unit time; the process throughput only accounts for the throughput of the fresh feed. In all cases, at the same values of R_c and R_b, continuous reflux had a higher column throughput than batch reflux. This higher column throughput associated with the continuous reflux also resulted in larger bed capacity factors and again contributed to the poorer performance of continuous reflux compared to batch reflux. Nevertheless, both reflux processes exhibited marked improvements over the conventional four-step Skarstrom-type cycle and even the five-step cycle with a cocurrent blowdown step.

Conclusions

New PSA-SVR cycle configurations were developed for increasing the heavy component (solvent vapor) enrichment, while still producing a very high purity light product. They include addition of a cocurrent blowdown step and combinations of a cocurrent blowdown step coupled with batch or continuous reflux steps to a typical four-step, Skarstrom-type cycle. A PSA-SVR process simulator was used to explore these new cycles and reveal the best configuration for PSA-SVR. Commercially relevant process conditions and column dimensions were used in the recovery of gasoline vapor with *n*-butane, *n*-heptane, and nitrogen as representatives of the light and heavy components in gasoline vapor and carrier gas, respectively. A high purity light product was produced in all cases.

Addition of a cocurrent blowdown step increased the solvent vapor enrichment with the extent depending mainly on the step end pressure and not the step time. Increasing the cocurrent blowdown step time had only a marginal, but favorable, effect on the solvent vapor enrichment. Decreasing the cocurrent blowdown step end pressure increased the solvent vapor enrichment, a favorable effect; it also increased the bed capacity factor, an unfavorable effect. Changes in the cocurrent blowdown step end pressure and step time had minimal effects on the temperature profiles in the column, a favorable result with respect to the bed capacity factor. Clearly, the addition of a cocurrent blowdown step in PSA-SVR processes has some distinct advantages for improving the solvent vapor enrichment, while at the same time producing a very high purity light product, as long as the columns are sized properly.

Both continuous and batch reflux steps coupled with a cocurrent blowdown step also increased the solvent vapor enrichment, with larger continuous reflux ratios or batch reflux time fractions producing larger increases. For example, both of the reflux cycles when combined with a cocurrent blowdown step increased the heptane vapor enrichment by more than 80% and the butane vapor enrichment by more than 60% compared to the basic, four-step cycle. These increases in the solvent vapor enrichment were at the expense of an increased bed capacity factor, however, which increased the possibility of solvent vapor breakthrough during the feed or cocurrent blowdown steps. Compared to the four-step cycle, larger bed capacity factors resulted in the five-step reflux cycles from increased solvent vapor concentrations at the column inlet during the feed step and from increased column throughputs. However, for similar increases in the solvent vapor enrichment, batch reflux led to smaller increases in the bed capacity factor compared to continuous reflux mainly due to lower feed concentrations and column throughputs. Larger increases in the column temperatures with continuous reflux compared to batch reflux also contributed to larger bed capacity factors.

Overall, batch reflux coupled with a cocurrent blowdown step produced a purer light product than continuous reflux under similar process conditions and solvent vapor enrichments. Thus, batch reflux was superior to continuous reflux in improving the process performance of the PSA-SVR processes. Nevertheless, adding a cocurrent blowdown step along with either batch or continuous reflux all improved the PSA-SVR process performance compared to the conventional four-step Skarstrom-type cycle.

Acknowledgments

The authors gratefully acknowledge financial support from the Exxon Engineering and Research Company, the Westvaco Charleston Research Center, and the Separations Research Program at the University of Texas at Austin.

Notation

A = area, m^2, or coefficient for the gas phase heat capacity, kJ/mol·K
B = coefficient for the gas-phase heat capacity, kJ/mol·K^2
b, b^o = adsorption isotherm parameters, kPa^{-1}

C = coefficient for the gas-phase heat capacity, kJ/mol·K^3
Cp_g = gas-phase heat capacity, kJ/mol·K
Cp_s = solid phase (pellet) heat capacity, kJ/kg·K
D = coefficient for the gas phase heat capacity, kJ/mol·K^4
E = solvent vapor enrichment
ΔH = isosteric heat of adsorption, kJ/mol
k = mass transfer coefficient, s^{-1}
L = bed length, m
M = molecular weight, kg/mol
q = solid-phase concentration (adsorbate loading), mol/kg
q^s = adsorption isotherm parameters, mol/kg
q^* = equilibrium amount adsorbed, mol/kg
r_b = column radius
R = gas constant, or solvent vapor recovery
T = temperature, K
T_o = ambient temperature, K
u = interstitial velocity, m/s
V_f = feed volumetric flow rate, m^3/min
y = gas-phase mole fraction
y_p = time averaged solvent vapor mole fraction in the light product
z = axial position in the column, m
ϵ = interstitial void fraction in the column
γ = volumetric purge to feed ratio

Subscripts

a = adsorbate
b = blowdown step or bed
bu = butane
c = cycle
e = effluent
f = feed
g = gas phase
hep = heptane
i = component
nit = nitrogen
p = pellet or light product

Literature Cited

Betlem, B. H. L., R. W. M. Gotink, and H. Bosch, "Optimal Operation of Rapid Pressure Swing Adsorption with Slop Recycling," *Computers Chem. Eng.*, **22**, 5633 (1998).

Brown, P. N., A. C. Hindmarsh, and L. R. Petzold, "Using Krylov Methods in the Solution of Large-Scale Differential-Algebraic Systems," *SIAM J. Sci. Comp.*, **15**, 1467 (1994).

Diagne, D., M. Goto, and T. Hirose, "New PSA Process with Intermediate Feed Inlet Position Operated with Dual Refluxes: Application to Carbon Dioxide Removal and Enrichment," *J. Chem. Eng. Jpn.*, **27**, 85 (1994).

Diagne, D., M. Goto, and T. Hirose, "Parametric Studies on CO_2 Separation and Recovery by a Dual Reflux PSA Process Consisting of Both Rectifying and Stripping Sections," *Ind. Eng. Chem. Res.*, **34**, 3083 (1995).

Dong, F., H. Lou, A. Kodama, M. Goto, and T. Hirose, "A New Concept in the Design of Pressure Swing Adsorption Processes for Multicomponent Gas Mixtures," *Ind. Eng. Chem. Res.*, **38**, 233 (1999).

Drago, R. S., D. S. Burns, and T. J. Lafrenz, "A New Adsorption Model for Analyzing Gas-Solid Equilibria in Porous Materials," *J. Phys. Chem.*, **100**, 1718 (1996).

Hall, T., and L. Larrinage, "Dow's Sorbathene Solvent Vapor Recovery Unit," I&EC Special Symp., American Chemical Society, Atlanta, GA (Sept., 1993).

Holman, R. J., and J. H. Hill, "New Development in Hydrocarbon Vapor Recovery," AIChE Meeting, Miami Beach, FL (Nov., 1992).

LeVan, M. D., "Pressure Swing Adsorption: Development of an Equilibrium Theory for Purification and Enrichment," *Ind. Eng. Chem. Res.*, **34**, 2655 (1995).

Liu, Y., and J. A. Ritter, "Pressure Swing Adsorption-Solvent Vapor Recovery: Process Dynamics and Parametric Study," *Ind. Eng. Chem. Res.*, **35**, 2299 (1996).

Liu, Y., and J. A. Ritter, "Fractional Factorial Study of a Pressure Swing Adsorption-Solvent Vapor Recovery Process," *Adsorption*, **3**, 151 (1997a).

Liu, Y., and J. A. Ritter, "Evaluation of Model Approximations in Simulating Pressure Swing Adsorption-Solvent Vapor Recovery," *Ind. Eng. Chem. Res.*, **36**, 1767 (1997b).

Liu, Y., and J. A. Ritter, "Periodic Heat Effects in Pressure Swing Adsorption-Solvent Vapor Recovery," *Adsorption*, **4**, 159 (1998).

Liu, Y., C. E. Holland, and J. A. Ritter, "Solvent Vapor Recovery by Pressure Swing Adsorption-I: Experimental Transient and Periodic Dynamics of the Butane-Activated Carbon System," *Sep. Sci. Technol.*, **33**, 2311 (1998a).

Liu, Y., C. E. Holland, and J. A. Ritter, "Solvent Vapor Recovery by Pressure Swing Adsorption-II: Experimental Periodic Performance of the Butane-Activated Carbon System," *Sep. Sci. Technol.*, **33**, 2431 (1998b).

Liu, Y., D. Subramanian, and J. A. Ritter, "Theory and Application of Pressure Swing Adsorption for the Environment," *Adsorption and Its Application in Industry and Environmental Protection: II. Applications in Environmental Protection*, A. Dabrowski, ed., Elsevier, Amsterdam, The Netherlands, p. 213 (1999a).

Liu, Y., C. E. Holland, and J. A. Ritter, "Solvent Vapor Recovery by Pressure Swing Adsorption-III: Comparison of Simulation with Experiments of the Butane-Activated Carbon System," *Sep. Sci. Technol.*, **34**, 1545 (1999b).

Liu, Y., J. A. Ritter, and B. K. Kaul, "Simulation of Gasoline Vapor Recovery by Pressure Swing Adsorption," *Sep. and Purification Technol.*, in press (2000).

Pezolt, D. J., S. J. Collick, H. A. Johnson, and L. A. Robbins, "Pressure Swing Adsorption for VOC Recovery at Gasoline Loading Terminals," *Env. Prog.*, **16**, 16 (1997).

Pigorini, G., and M. D. LeVan, "Equilibrium Theory for Pressure Swing Adsorption. 3. Separation and Purification in Two-Component Adsorption," *Ind. Eng. Chem. Res.*, **36**, 2306 (1997).

Ritter, J. A., and R. T. Yang, "Pressure Swing Adsorption: Experimental and Theoretical Study on Air Purification and Vapor Recovery," *Ind. Eng. Chem. Res.*, **30**, 1023 (1991a).

Ritter, J. A., and R. T. Yang, "Air Purification and Vapor Recovery by Pressure Swing Adsorption: Comparison of Silicalite and Activated Carbon," *Chem. Eng. Commun.*, **108**, 289 (1991b).

Ritter, J. A., and Y. Liu, "Tapered Pressure Swing Adsorption Columns for Simultaneous Air Purification and Solvent Vapor Recovery," *Ind. Eng. Chem. Res.*, **37**, 2783 (1998).

Ritter, J. A., Y. Liu, and D. Subramanian, "New Vacuum Swing Adsorption Cycles for Air Purification with the Feasibility of Complete Cleanup," *Ind. Eng. Chem. Res.*, **37**, 1970 (1998).

Ruthven, D. M., *Principles of Adsorption and Adsorption Processes*, Wiley, New York (1984).

Ruthven, D. M., S. Farooq, and K. S. Knaebel, *Pressure Swing Adsorption*, VCH Publishers, New York (1994).

Ruthven, D. M., and S. Farooq, "Concentration of A Trace Component by Pressure Swing Adsorption," *Chem. Eng. Sci.*, **49**, 51 (1994).

Subramanian, D., and J. A. Ritter, "Equilibrium Theory for Solvent Vapor Recovery by Pressure Swing Adsorption: Analytical Solutions for Process Performance," *Chem. Eng. Sci.*, **52**, 3147 (1997).

Subramanian, D., and J. A. Ritter, "Equilibrium Theory for Binary Solvent Vapor Recovery by Pressure Swing Adsorption: Conceptual Process Design for Separation of the Light Component," *Chem. Eng. Sci.*, **53**, 1295 (1998).

Subramanian, D., J. A. Ritter, and Y. Liu, "Equilibrium Theory for Solvent Vapor Recovery by Pressure Swing Adsorption: Analytical Solutions with Velocity Variation and Gas-Phase Capacity," *Chem. Eng. Sci.*, **54**, 475 (1999).

Suh, S. S., and P. C. Wankat, "Combined Cocurrent-Countercurrent Blowdown Cycles in Pressure Swing Adsorption," *AIChE J.*, **35**, 523 (1989a).

Suh, S. S., and P. C. Wankat, "A New Pressure Swing Adsorption Process for High Enrichment and Recovery," *Chem. Eng. Sci.*, **44**, 567 (1989b).

Yang, R. T., *Gas Separation by Adsorption Processes*, Butterworths, Boston (1987).

Yoshida, M., A. Kodama, M. Goto, and T. Hirose, "Enrichment of Useful Trace Components in Air by New PSA Process," *Fundamentals of Adsorption 6*, M. Meunier, ed., Elsevier, Paris, p. 817 (1998).

Manuscript received Aug. 2, 1999, and revision received Oct. 25, 1999.